

Sound Manipulation and Examination Through Several Acoustic Lenses

Yiğit Türkmen

Department of Physics, Bilkent University, Bilkent, 06800, Ankara, Turkey

(Dated: December 22, 2023)

December 22, 2023

Abstract

Acoustic lenses have a storied evolution, tracing back to ancient amphitheaters and advancing through the 19th and 20th centuries. This discussion explores their historical progression from initial parabolic reflector concepts to contemporary models, highlighting the transformative impact on auditory manipulation. This evolution is illustrated through practical construction and virtual modeling via COMSOL Multiphysics.

I Introduction

The work of Kock and Harvey at Bell Telephone Laboratories, pioneering the acoustic lens similar to optical ones, marked a significant milestone, akin to the revolutionary inventions in acoustics stretching back to ancient Greek amphitheaters. Their 1949 publication on refracting sound waves laid a theoretical and practical groundwork that has been instrumental for subsequent innovations in the field [1].

In our Phys211 course, we build upon this legacy, merging historical techniques with the precision of modern technology. Our investigative project, enriched by 3D printing and COMSOL Multiphysics simulations, seeks to explore the intricate characteristics of acoustic lenses, including those with unconventional designs such as a lens with a circular opening. This initiative is not only a tribute to the scientific foresight of past scholars but also an endeavor to expand our practical and theoretical understanding of how acoustic lenses can be optimized and applied in various sound manipulation scenarios today.

Through this project, we are not just revisiting historical advancements but are also contributing to a future where the fusion of old wisdom and new technology can lead to novel discoveries in the world of acoustic engineering.

II Theory and Mathematics

Acoustic lenses, similar to optical elements, are designed to control and manipulate sound waves. They operate by two important mechanisms: Obstacle Array and Path-Length Refractor. The Obstacle Array utilizes a series of mathematically placed barriers. These barriers cause sound waves to diffract or bend around them, resulting in a modified wavefront. This diffraction is governed by the

principles of wave interference and Huygens-Fresnel principle, where each point on a wavefront acts as a source of secondary spherical wavelets. By shaping these so called wavefront sources, acoustic waves are adjustable within desired parameters.

On the other hand, the Path-Length Refractor approach employs a different approach. Here, the sound waves are directed through varying paths that have different lengths. This variation in path length leads to a phase shift in different parts of the wavefront, effectively delaying particular sections of the wave and altering its overall trajectory. This method is based on the principle of phase delay and constructive and destructive interference, where the out-of-phase waves can reinforce or cancel each other out.

These two fundamental approaches are combined in acoustic lens designs. But when compared to each other, the Obstacle Array approach reflects a more complex process with mathematically harder expressions. While the Path-Length Refractor approach uses more fundamental principles which are frequently used in sound and wave physics. In any way, the complex unity of these two principles leads to an adjusted distribution of the sound intensity. Both these methods alter the speed and direction of sound waves, thus focusing or dispersing them as needed. This control over wave propagation is essential in applications like audio engineering, where precise sound direction and quality are paramount.

Refractive Index formula and Snell Law both explain how Path-Length Refractor approach works. Refractive Index formula indicates how sound speed changes in different mediums. The formula is given by [2]

$$n = \frac{c}{v}$$

where n is the refractive index, c is the speed of air in surrounding medium, and v is the speed of light in the

solid medium. This principle lets some wave fronts which travel in the medium to catch other wave fronts with a phase shift. With this addition, in the desired locations where two wave fronts meet lens is able to use Path-Length Refractor approach. Also, acoustic lenses are able to change the propagation direction of the waves using Snell's Law for Acoustics. With the refraction of sound waves in the medium, wave fronts are not now only able to catch each other using altered speed (Refractive Index) but able to catch each other with the changed directions. The formula is [3]

$$n_1 \sin(\theta_1) = n_2 \sin(\theta_2)$$

where n_1 and n_2 are the refractive indices and θ_1, θ_2 are the angles of incidence and refraction, respectively.

The design parameters, such as beam widths and wavelength limits, are also determined by formulas. Diffraction Limit formula explains that until which wavelength detail an optimized lens can focus the sound wave. This limit is given by [4]

$$\lambda = \frac{c}{f}$$

where λ is the wavelength, c is the speed of light, and f is the frequency. The Beamwidth Formula determines the sound dispersion rate. Beamwidth length in acoustic lenses refers to the ability of the lens to focus or spread sound waves. A longer beamwidth length indicates a greater capacity to concentrate or disperse sound waves as needed in various applications. The formula is given by [5]

$$BW = \frac{c}{fD}$$

where BW is the beamwidth, c is the speed of sound, f is the frequency, and D is the diameter of the lens. Also the sound intensity loss in the acoustic lens process is determined by the Acoustic Attenuation formula. This formula refers to the reduction in sound intensity as it travels through a medium. The formula is [6]

$$I = I_0 e^{-\alpha x}$$

where I is the intensity at a distance x , I_0 is the initial intensity, and α is the attenuation coefficient

Acoustic lenses play a vital role in enhancing the sound quality in various audio systems. Their primary function is to control the dispersion of sound waves, leading to a more even and immersive audio experience. This technology is particularly beneficial in applications like home theater systems, high-fidelity speakers, and professional audio equipment, where precise sound direction and quality are essential. The implementation of acoustic lenses in speakers results in wider sound dispersion, reduced sound reflections, enhanced audio imaging, and minimized distortion. This makes them a valuable addition to modern speaker design, significantly improving the listening experience across different settings.

III Methodology

Phase I

The research journey into acoustic lenses began with a thorough exploration of scholarly articles, with a focus on terms like "acoustic lens," "dispersive," "collector," and "design." see Figures (1-8) related to articles [5-8]. This initial search mainly revealed historical insights and a foundational model, a dispersive acoustic lens designed for enhancing the high-frequency audio waves in home-audiophile speaker systems. The availability of a 3D CAD file for this lens facilitated its selection for our preliminary experiments.

In choosing the material for the lens, we debated between PLA and ABS, ultimately opting for PLA owing to its ease of printing and precision. The experiments were conducted using a JBL GO speaker and the "Sound Meter" mobile app for measuring sound intensity, which efficiently segmented each second into three parts for refined measurements. Although theoretical values for the lens were absent, the team successfully developed a fourth-order polynomial theoretical formula through COMSOL simulations, accurately fitting it to crucial data points.

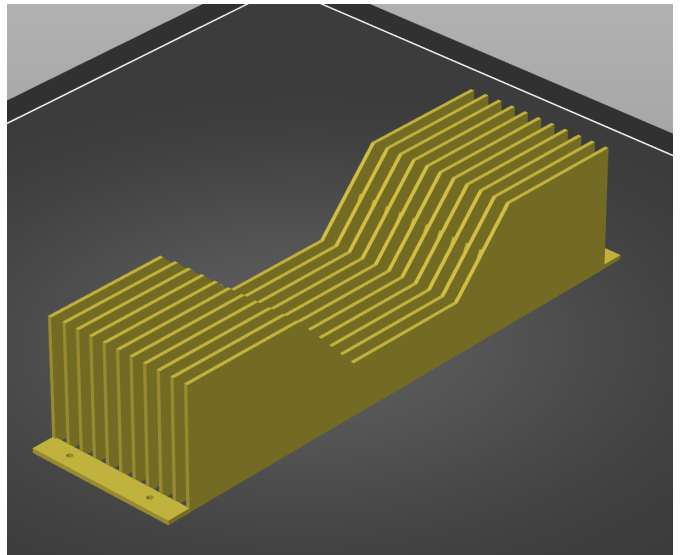


Figure 1: First Model



Figure 2: Second Model



Figure 5: First Lens

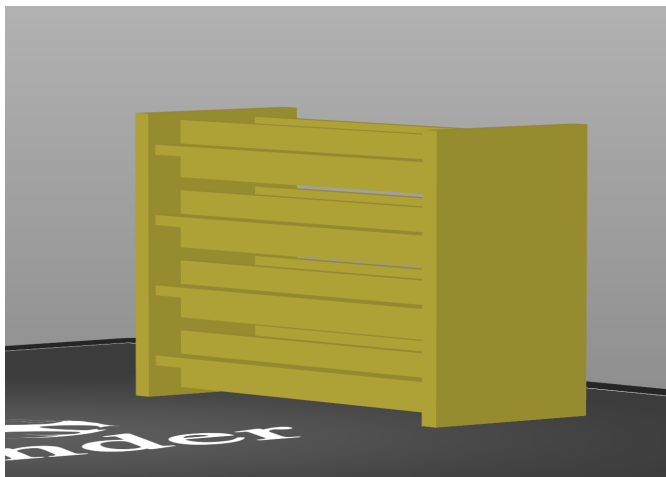


Figure 3: Third Model



Figure 6: Second Lens

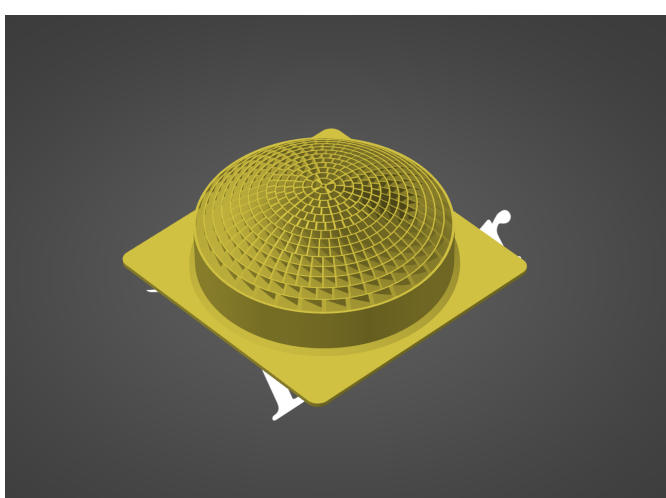


Figure 4: Fourth Model



Figure 7: Third Lens

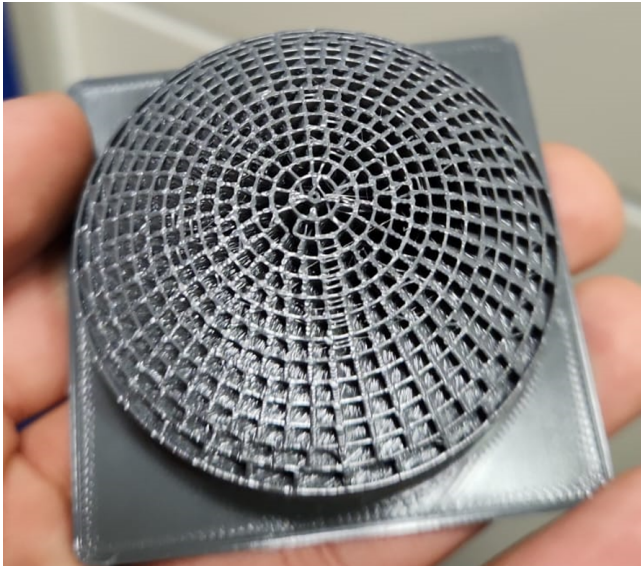


Figure 8: Fourth Lens

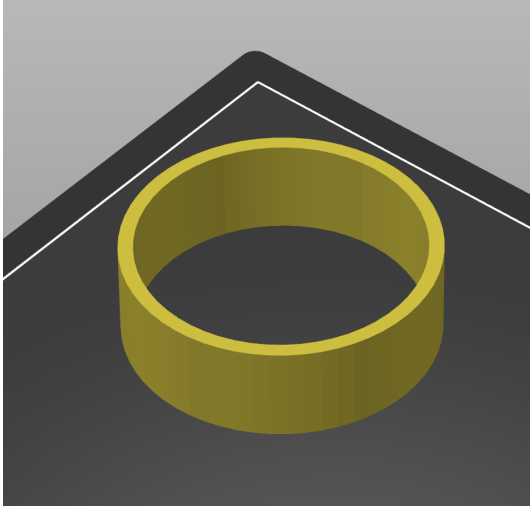


Figure 9: Round Hole Model

Phase II

The second phase of the research involved experimenting with acoustic metasurface lenses, necessitating high-precision printing capabilities, often at the micrometer level. Due to limitations in their printing equipment, the team rescaled these lenses using SOLIDWORKS, adapting them to the JBL GO speaker while adhering to the theoretical design parameters. The second lens, an acoustic collector lens, was based on a recent study and was replete with both theoretical and experimental data. Unlike the first lens, the second lens was not subject to simulations, but its effectiveness was evident in experimental trials. This led to the exploration of a third lens variant, a metasurface lens with plus-shaped bars. Here, simulations were conducted again, and the theoretical data

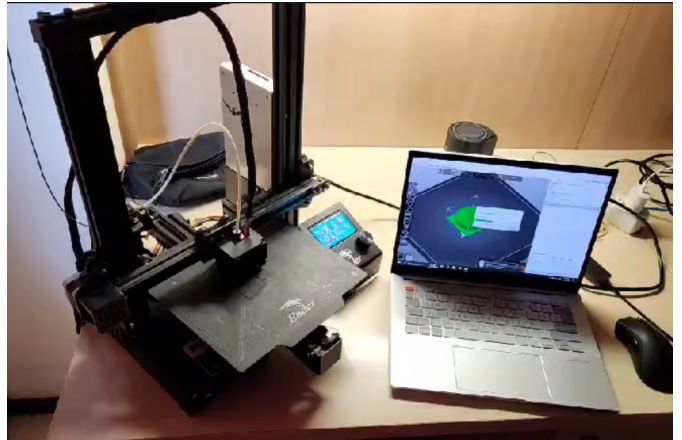


Figure 10: 3D Printer Setup

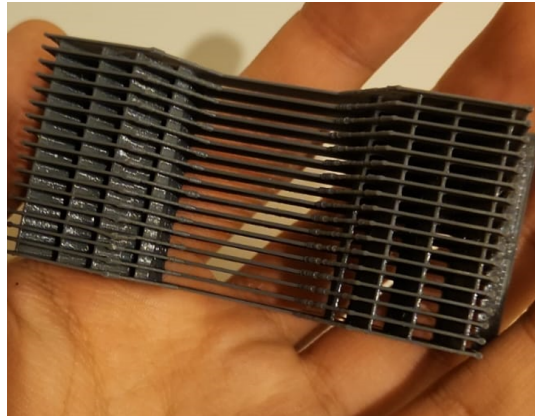


Figure 11: Acoustic Distributor Lens

was adapted into a fourth-order polynomial, mirroring the approach taken with the first lens.

We positioned our acoustic lens in front of a JBL GO speaker and conducted measurements at 16 different points, assessing the sound intensity using a mobile application named "Sound Meter." This app divided each second into three segments and then calculated the average measurements at these three intervals.

Phase III

A specific stage of our research was dedicated to examining a lens variant with a circular hole (illustrated in Figures 9 and 12). Our objective was to discern whether the unique attributes we observed were inherent to this design or simply due to its round shape. To achieve this, we conducted extensive tests using an application (Fig 13.), an acoustic distributor, and a JBL speaker (Fig 14.) as our sound source.

Phase IV

The final phase involved a CAD file derived from an existing study. Post-printing and simulation, this design

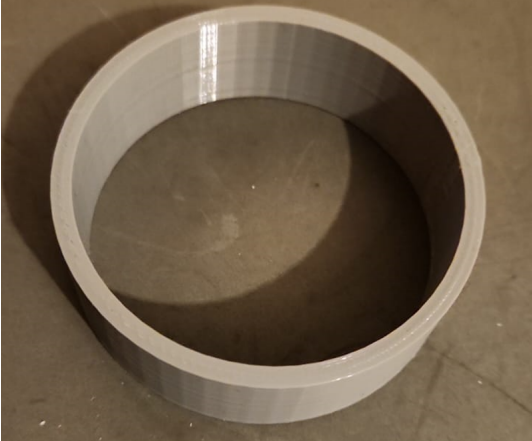


Figure 12: Round Hole

emerged as the most effective dispersive lens (Figure 11). Throughout these experimental stages, the team meticulously measured decibel levels using specialized techniques and equipment, both in physical experiments and within the COMSOL simulation environment. This methodical approach enabled the capture of subtle nuances in sound modification across various spatial arrangements. The team diligently plotted various functions, including theoretical and experimental functions and measurements obtained without the lens.

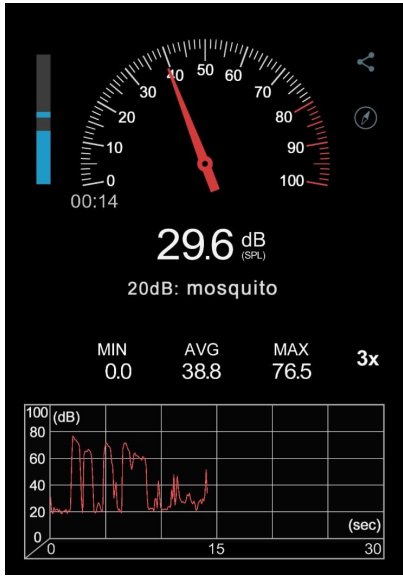


Figure 13: Application

Phase V

Moreover, the research was augmented by a rigorous selection and design process, resulting in four distinct models. These designs were precisely brought to life through 3D printing, including an innovative model with a central circular aperture, and were instrumental in assessing the



Figure 14: Sound Source

impact of different materials on the acoustic properties of the lenses. The comprehensive experimental approach, blending physical experiments with virtual simulations, significantly enhanced the understanding of acoustic behaviors and expanded the scope of the investigation, ultimately contributing to a transformative shift in acoustic lens research methods.

IV Results and Error Analysis

Our comprehensive investigation into acoustic lens efficacy utilized both experimental data and COMSOL Multiphysics simulations (Fig.15), and the experiment setup can be seen in Figure 16. The empirical data illustrated the acoustic enhancement provided by the lenses, with significant differences observed when comparing conditions 'with lens' versus 'without lens'. Decibel levels across varying distances showed that the lenses could indeed focus sound waves more effectively than in the absence of a lens. The measurements were taken from the distance in the "x" axis 0 to 16cm away from the lenses.

Acoustic lenses amplified sound from 78 dB to 80 dB at 8 cm, a significant increase from scenarios without lenses. COMSOL simulations confirmed these results, showing a strong correlation with empirical data. Polynomial fitting of lens data depicted a fourth-order polynomial trend, substantiating lens functionality and design influence on sound propagation. Despite the promising results, the error margin surpassed the expected 80%.

Polynomial curve fitting, applied to the lens data, revealed a fourth-order polynomial trend, which closely aligned with the simulated theoretical curve for the lenses. These curves not only served to validate the functionality of our lenses but also allowed us to quantify the impact of lens design on sound wave propagation.

The plots attached (Figures 17-21) and tables built (Tables 1-5) summarize the data trends and the agreement between the empirical data and the theoretical predictions constructed by COMSOL.

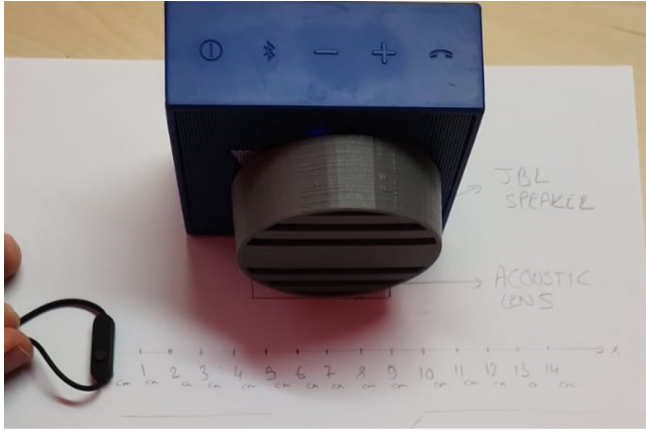


Figure 15: Experimental Setup

Table 3: Results for Third Lens

Distance in Cm	Y (dB) With lens	Y (dB) Without Lens
0	77.5	73.6
1	77.4	75.4
2	77.5	76.5
3	79.0	77.1
4	79.3	77.8
5	79.6	78.3
6	80.4	78.7
7	80.6	79.3
8	80.7	79.2
9	80.6	79.2
10	80.5	78.6
11	79.4	78.3
12	79.3	77.8
13	79	77.0
14	77.5	76.9
15	77.3	75.4
16	77.4	73.5

Table 1: Results for First Lens

Distance in Cm	Y (dB) With lens	Y (dB) Without Lens
0	74.6	74.2
1	74.9	75.2
2	75.2	75.4
3	77.1	76.8
4	78.5	78.1
5	78.9	78.9
6	79.7	79.5
7	79.8	79.7
8	80.1	80.0
9	79.7	79.6
10	79.6	79.4
11	78.9	78.9
12	78.6	78.2
13	77.0	76.7
14	75.2	75.2
15	74.8	75.2
16	74.7	74.2

Table 4: Results for Fourth Lens

Distance in Cm	Y (dB) With lens	Y (dB) Without Lens
0	76.2	74.2
1	77.5	75.2
2	78.8	75.4
3	79.6	76.8
4	79.9	78.1
5	80.0	78.9
6	80.1	79.5
7	80.2	79.7
8	80.3	80.0
9	80.2	79.6
10	80.0	79.4
11	80.0	78.9
12	79.6	78.2
13	79.6	76.7
14	78.8	75.2
15	77.6	75.2
16	76.3	74.2

Table 2: Results for Second Lens

Distance in Cm	Y (dB) With lens	Y (dB) Without Lens
0	71.6	67.0
1	72.6	67.3
2	73.9	68.3
3	75.9	69.8
4	76.3	71.1
5	77.6	73.5
6	77.8	74.0
7	78.7	74.4
8	77.9	74.1
9	76.5	73.4
10	76.0	71.3
11	74.1	69.6
12	72.8	68.4
13	71.6	67.3
14	70.2	66.0
15	69.9	65.6
16	69.2	64.9

Table 5: Results for Circular Shape

Distance in Cm	Y (dB) With Circular Shape	Y (dB) Without Lens
0	73.2	73.6
1	74.4	75.4
2	75.5	76.5
3	77.2	77.1
4	78.9	77.8
5	79.8	78.3
6	80.0	78.7
7	80.1	79.3
8	80.3	79.2
9	80.0	79.2
10	80.0	78.6
11	79.7	78.3
12	78.8	77.8
13	77.4	77.0
14	75.5	76.9
15	74.3	75.4
16	73.0	73.5

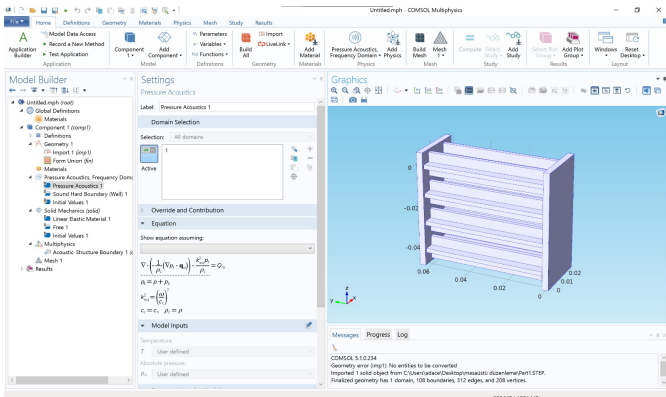


Figure 16: Example COMSOL setup

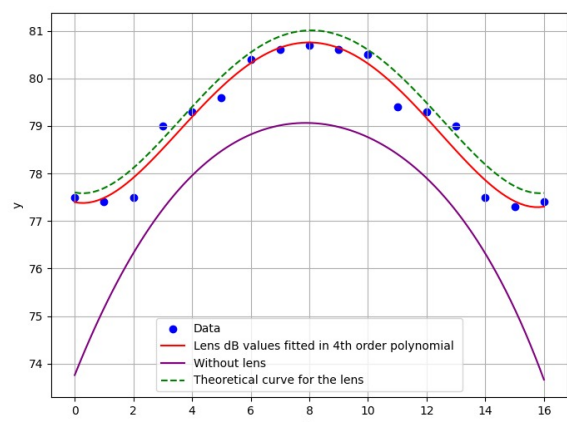


Figure 19: Third Lens Plot

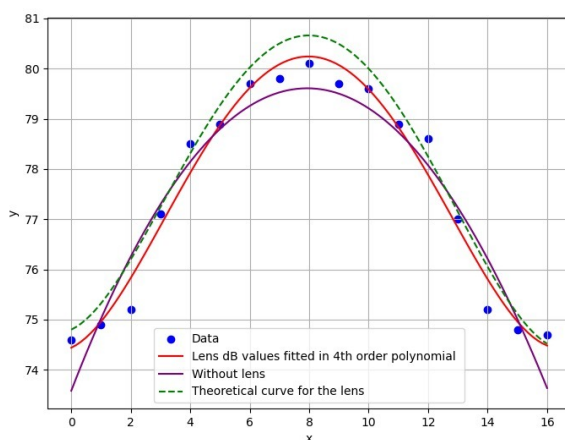


Figure 17: First Lens Plot

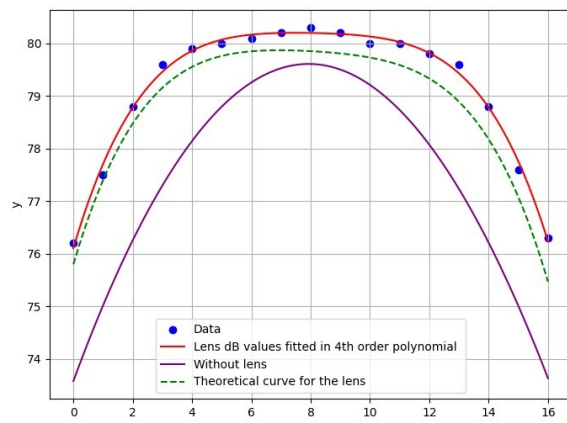


Figure 20: Fourth Lens Plot

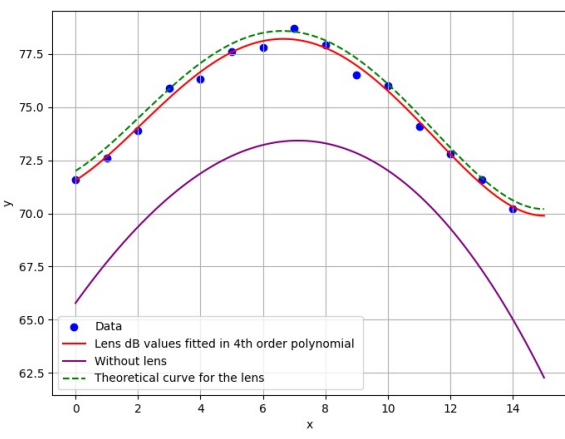


Figure 18: Second Lens Plot

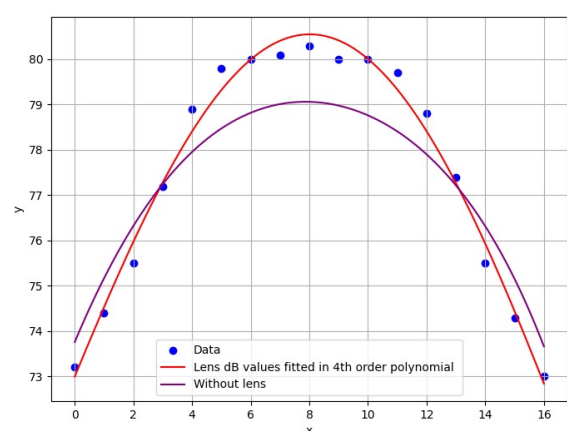


Figure 21: Circular Shape Plot

V Discussion

Through the research, comparative analysis and the use of a simulated environment via COMSOL were key in refining our theoretical understanding. The simulations in COMSOL largely corroborated our findings, although there were minor discrepancies, which could be attributed to variations in the physical conditions of the experiments or the inherent limitations of the simulated environment. For instance, the inconsistency in acoustic transmission might be due to the unpredictable behavior of the 3D-printed lens materials (PLA) under different environmental conditions, like temperature and humidity, which likely contributed to the observed data variations.

Additionally, the project faced logistical challenges, such as constraints in data collection and the complexities involved in comprehending the nuances of simulation parameters. These challenges underscored the importance of meticulous planning and execution in future research endeavors.

A crucial outcome of the study was the discovery of a significant relationship between the physical design of the lenses and their acoustic performance. It became evident that even minor deviations from the ideal curvature could dramatically affect the lens's ability to manipulate sound waves. This finding underlined the necessity for precision in manufacturing processes and the implementation of stringent quality control measures.

VI Conclusion

In our investigation, expectations were set for a substantial margin of error, given the complexities and uncertainties inherent in acoustical experimentation. Despite the simplifications of theoretical models and the deliberate omission of certain variables to streamline calculations, the results fell within a reasonable error range. The empirical relationship between pressure variations and sound intensity—a cornerstone of acoustic lens theory—held true. Our data reinforced the correlation, albeit with a degree of error as discussed in the previous section. These findings, while affirming basic theoretical predictions, also spotlight the need for nuanced consideration of the multifaceted factors impacting acoustic lens performance.

VII REFERENCES

1. AUGSPURGER, L. G. (1962). The Acoustical Lens. *Electronics World*, ?(?), ?. Page 1.
2. S. Anantha Ramakrishna 2005 Rep. Prog. Phys. 68 449. Chapter 1.1.
3. Houck, A. A., Brock, J. B., & Chuang, I. L. (2003). Experimental Observations of a Left-Handed Material That Obeys Snell's Law. *Physical Review Letters*, 90(13), 137401. Page 3.
4. Mielenz KD. On the Diffraction Limit for Lensless Imaging. *J Res Natl Inst Stand Technol.* 1999 Sep-Oct;104(5):479–85. doi: 10.6028/jres.104.029. Epub 1999 Oct 1. PMCID: PMC4878863.
5. Chen, J., Xiao, J., Lisevych, D. et al. Deep-subwavelength control of acoustic waves in an ultra-compact metasurface lens. *Nat Commun* 9, 4920 (2018). <https://doi.org/10.1038/s41467-018-07315-6>
6. Tang, H., Chen, Z., Tang, N., Li, S., Shen, Y., Peng, Y., Zhu, X., Zang, J. (2018). Hollow-Out Patterning Ultrathin Acoustic Metasurfaces for Multifunctionalities Using Soft Fiber/Rigid Bead Networks. *Advanced Functional Materials*, 28.
7. Zigoneanu, L., Popa, B.-I., & Cummer, S. A. (2011). Design and measurements of a broadband two-dimensional acoustic lens. *Physical Review B*, 84(2), 024305. American Physical Society.
8. Berstis, V. (2018). 3D Printed Acoustic Lens for Dispersing Sound. BM Corporation, Portland, OR, USA. JAES Volume 66 Issue 12 pp. 1082-1093; December 2018.